Organocatalysis

DOI: 10.1002/ange.201101385

Brønsted Acid Catalysis: Hydrogen Bonding versus Ion Pairing in Imine Activation**

Matthias Fleischmann, Diana Drettwan, Erli Sugiono, Magnus Rueping, and Ruth M. Gschwind**

Despite the crucial role of hydrogen-bonding interactions and proton transfer in organocatalysis, especially in the reactions involving Brønsted acid catalysts,[1] fundamental understanding of the nature of catalyst–substrate complexes in solution is rather limited. One reason for the challenges associated with investigation of the catalytically active species in Brønsted acid catalysis is their lack of experimental accessibility. This difficulty is valid in particular for 1,1′-binaphthalene-2,2′-diol (binol) phosphoric acids,[2–4] with which the activation of the substrate takes place either through proton transfer or hydrogen bonding, with or without charge assistance by the catalyst. To improve the catalytic performance of Brønsted acid catalysts it is essential to identify the different catalytic species present in solution. Schrader et al. were able to detect key intermediates in a cascade reaction involving a binol-derived phosphoric acid catalyst by electrospray ionization mass spectroscopy (ESI-MS).[5] However, with this method, it was not possible to differentiate between proton transfer and hydrogen-bond formation. Owing to our tremendous interest in the further development of binol-derived phosphoric acids and derivatives as efficient Brønsted acid catalysts for application in various transformations involving imines,[2,4] we decided to conduct experiments which would help identify the activation mode in these reactions.

NMR spectroscopy has emerged as a powerful technique for the investigation of both hydrogen-bonding and ion-pair systems.[6] Limbach and co-workers showed in marvelous studies on the hydrogen-bond networks in various pyridoxal 5′-phosphate derived Schiff bases that the intermolecular hydrogen bonds could be characterized by a combination of ^{1}H and ^{15}N NMR spectroscopy.[7–10] A correlation between the ^{1}H and ^{15}N chemical shifts, the corresponding coupling constants $^{1}J_{H,N}$, and the hydrogen-bond strength was found. In principle, the direct detection of 1D, 2D, and 3D correlations caused by intermolecular $^{2h}J_{H,P}$ and $^{1h}J_{H,N}$ couplings is possible; however, sharp line widths, which indicate slow relaxation, are required. Only few studies dealing with the detection of magnetization transfer through hydrogen bonds in non-biomolecules in organic solvents have been reported. For example, we investigated artificial arginine and acylguanidine complexes by NMR spectroscopy.[11,12] Hence, we chose NMR spectroscopy as an adequate tool to identify the species present in various Brønsted acid/imine mixtures and to examine the influence of temperature and concentration on imine protonation.[13,14]

The model compounds selected for our investigations are depicted in Scheme 1. Diphenyl phosphate (DPP, **1**, $pK_a < 2$) was selected as an achiral phosphate used in Brønsted acid catalyzed transformations.[2–4] Imines **2** and **3** were selected as substrates for identification of the main trends between aldimines and ketimines. The effect of electron density was investigated with the aid of ketimines **3** and **4** bearing aromatic substituents with different electronic properties. To select the optimal experimental conditions, we investigated the NMR spectroscopic properties of the complex **1·2** in dichloromethane, chloroform, and toluene, the typical solvents used in synthetic applications.[2–4] Toluene was found to provide by far the best chemical shift dispersion and solubility. To enable the detection of the hydrogen-bonding properties of the analyzed complexes **1·2**, **1·3**, and **1·4**, 1:1 mixtures of the phosphate and the imine were used, and the highest possible concentration was chosen for each individual complex (100, 40, and 20 mM, respectively).[15] To enable the determination of $^{1}J_{^{15}N,^{1}H}$ coupling constants and to facilitate ^{1}H,^{15}N magnetization transfer, we synthesized ^{15}N-labeled imines **2**–**4**. Since

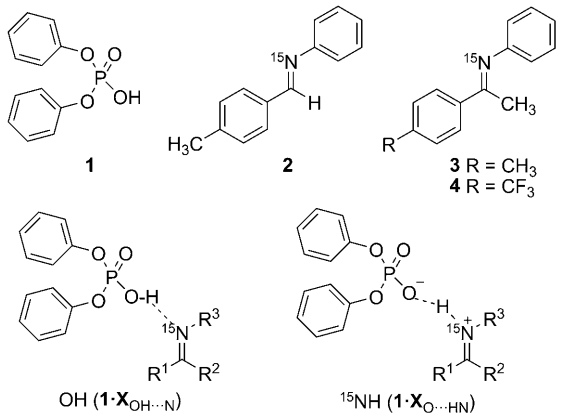

Scheme 1. Investigated model systems with the acid catalyst diphenyl phosphate (**1**) and different imines **2**–**4**.

[*] M. Fleischmann, D. Drettwan, Prof. Dr. R. M. Gschwind
Institut für Organische Chemie, Universität Regensburg
Universitätsstrasse 31, 93053 Regensburg (Germany)
Fax: (+49) 941-943-4617
E-mail: ruth.gschwind@chemie.uni-regensburg.de
Dr. E. Sugiono, Prof. Dr. M. Rueping
Institut für Organische Chemie, RWTH Aachen
Landoltweg 1, 52074 Aachen (Germany)
Fax: (+49) 241-809-2665
E-mail: magnus.rueping@rwth-aachen.de

[**] This research was supported by the DFG (SPP 1179).
Supporting information for this article is available on the WWW under http://dx.doi.org/10.1002/anie.201101385.

WILEY ONLINE LIBRARY
© 2011 Wiley-VCH Verlag GmbH & Co. KGaA, Weinheim

the NMR spectra of the three complexes investigated were very similar, the NMR spectroscopic approach used to identify the position of the crucial proton is explained exemplarily for complex **1·2**. All NMR spectroscopic data of **1·2**, **1·3**, and **1·4** are summarized in Table S1 in the Supporting Information.

At 300 K, the ^{1}H NMR spectrum of **1·2** showed only one averaged signal for the acidic proton (Figure 1 a). Therefore, we carried out low-temperature studies to identify chemical-exchange processes, which are highly probable at room temperature between the proposed species formed by intermolecular hydrogen bonding and proton-transfer species. Indeed, below 280 K, three signals were observed for the acidic proton. These signals become sharper as the temperature was decreased to 240 K (Figure 1 a), at which temperature a singlet at $\delta = 18.16$ ppm and two doublets at $\delta = 15.50$ and 11.87 ppm with $^1J_{H,N}$ coupling constants of 86.0 ± 1 and 69.5 Hz were observed.[16] Upon further cooling, each of the two signals above 15 ppm split into a group of signals, which indicated similar binding properties of the acidic proton but structurally slightly deviating species. In contrast, in the ^{31}P NMR spectrum, only one averaged singlet was observed at all temperatures (Figure 1 b).

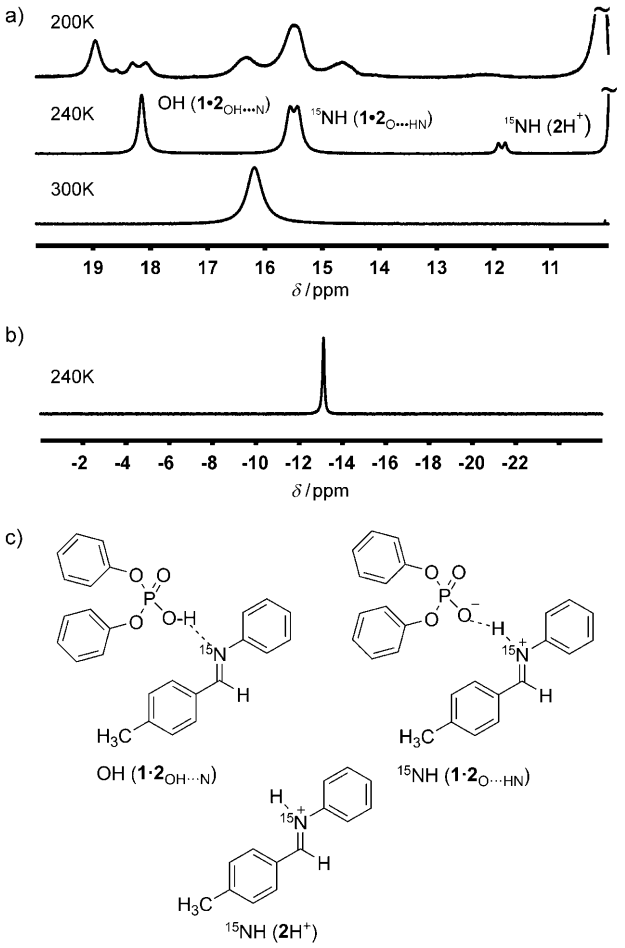

Figure 1. a) Temperature dependence of the ^{1}H NMR spectra of **1·2**. b) ^{31}P NMR spectrum of **1·2** at 240 K in [D_8]toluene at 600 MHz. c) Identified species.

In the temperature study, extremely broad proton signals (line widths up to 480 Hz) were detected (see Figure 1 a; see also the Supporting Information). This broadness indicates very short transversal relaxation times and exchange, which severely hamper the detection of magnetization transfer as required for the differentiation of hydrogen-bonded and proton-transfer complexes. Therefore, for the subsequent NMR spectroscopic investigations, we chose a temperature of 240 K, which provides the smallest line widths (165, 105, and 50 Hz) and shows one averaged signal for each of the three main species (Figure 1 c). In principle, it should be possible to identify the bonding properties of the acidic proton in these three species from ^{1}H,^{31}P HMBC and ^{1}H,^{15}N HMQC spectra. For POH compounds, ^{1}H,^{31}P HMBC crosspeaks are expected, and for HN$^+$ compounds, ^{1}H,^{15}N HMQC crosspeaks should be observed. Indeed, two crosspeaks were detected in the ^{1}H,^{15}N HMQC spectrum (Figure 2 c). These crosspeaks enabled the assignment of the signals at $\delta = 15.50$ and 11.87 ppm to HN$^+$ species. For the third proton signal at $\delta = 18.16$ ppm, no crosspeak was observed despite extensive magnetization-transfer-delay optimizations in various ^{1}H,^{15}N HMBC experiments and experimental times up to 10 h. No crosspeaks were observed in the corresponding ^{1}H,^{31}P HMBC spectra even when various spectroscopic parameters were used. This lack of crosspeaks can be explained by the short transversal relaxation times of the three proton signals in combination with small $^2J_{H,P}$ coupling constants. Therefore, we carried out time-shared ^{31}P,^{1}H INEPT experiments (INEPT = insensitive nuclei enhanced by polarization transfer), which show significantly higher signal-to-noise ratios for systems with long ^{31}P T_2 times and short ^{1}H T_2 times.[11] However, even in transfer-delay-optimized ^{31}P,^{1}H INEPT spectra with experimental times around 10 h, only one crosspeak to the signal at

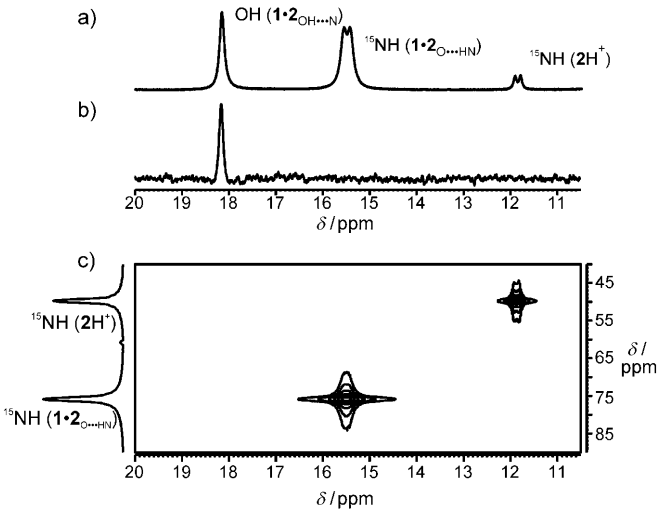

Figure 2. NMR spectroscopic characterization of the 1:1 complex of **1** and **2** at 240 K in [D_8]toluene at 600 MHz: a) OH region of the ^{1}H NMR spectrum indicating three different species; b) 1D ^{31}P,^{1}H INEPT spectrum; c) 2D ^{1}H,^{15}N HMQC spectrum.

 © 2011 Wiley-VCH Verlag GmbH & Co. KGaA, Weinheim

$\delta = 18.16$ ppm was detected (Figure 2b). These $^{1}H,^{15}N$ HMQC and $^{31}P,^{1}H$ INEPT spectra show that in a 1:1 mixture of **1** and **2**, one POH and two HN^+ species exist simultaneously, and that the detection of magnetization transfer through potential hydrogen bonds in these species is hampered by short ^{1}H relaxation times and small ^{nh}J values.

First, the POH species ($\delta(^{1}H) = 18.16$ ppm) was identified. In principle, this signal could either belong to **1** or to the expected OH(**1**·**2**$_{OH\cdots N}$) complex (Figure 1c). To differentiate between these two possibilities, we investigated the chemical shifts and aggregation levels of the pure catalyst **1** and compared them to those of the **1**·**2** sample. At 240 K, pure **1** showed a significantly high-field-shifted OH signal at $\delta(^{1}H) = 13.80$ ppm, which is close to the value for dimethyl phosphate.[17] This signal did not split into several signals at temperatures below 240 K as found for **1**·**2** (for spectra, see the Supporting Information). Furthermore, diffusion measurements showed different values for **1** and OH(**1**·**2**$_{OH\cdots N}$), and when the temperature was lowered for **1**, a trend from the formation of dimers to the formation of trimers was observed, as similarly reported for dimethyl phosphate (for details, see the Supporting Information).[17] Therefore, the presence of pure **1** in the **1**·**2** sample can clearly be excluded.

For the POH species in the **1**·**2** sample, the diffusion values were in agreement with the formation of a **1**·**2** complex (for details, see the Supporting Information), which we refer to herein as the DPP–aldimine complex OH(**1**·**2**$_{OH\cdots N}$) (Figure 1c). The remarkable downfield shift of the OH proton signal in the spectrum of OH(**1**·**2**$_{OH\cdots N}$) compared to the OH proton signal of the **1**·**1** dimer suggests the presence of a stronger hydrogen bond in OH(**1**·**2**$_{OH\cdots N}$) than in the **1**·**1** dimer. However, anisotropy effects of the aldimine substituents in OH(**1**·**2**$_{OH\cdots N}$) may also contribute to the observed chemical shift difference.

Next, the two HN^+ species were assigned. In principle, these signals could belong to **2**H^+, **2**·**2**H^+, or the expected NH(**1**·**2**$_{O\cdots HN}$) complex (Figure 1c). To differentiate between these possibilities, we simulated the chemical shifts and/or aggregation levels of **2**H^+ and **2**·**2**H^+ with samples of **2** combined with 1.0 and 0.5 equivalents of HBF_4, respectively. The experiments with **2** and one equivalent of HBF_4 resulted in a proton signal for **2**H^+ at $\delta = 11.39$ ppm, very close to that at $\delta = 11.87$ ppm for the **1**·**2** sample. This result indicates the existence of the free protonated aldimine NH(**2**H^+) in the **1**·**2** sample (Figure 1c; for spectra, see the Supporting Information). The presence of NH(**2**H^+) was confirmed by ^{1}H DOSY NMR experiments, which revealed a temperature- and viscosity-corrected diffusion coefficient of $D_{corr}(NH(\mathbf{2}H^+)) = 4.40 \times 10^{-10}\ m^2 s^{-1}$, indicative of a monomeric aldimine. The experiments with **2** and 0.5 equivalents of HBF_4 resulted in a proton signal at $\delta = 12.14$ ppm for the **2**·**2**H^+ complex. This chemical shift is close to that observed for monomeric **2**H^+; however, a downfield shift by 3.36 ppm was observed for the second HN^+ signal observed in the **1**·**2** sample at $\delta = 15.50$ ppm. Therefore, the formation of **2**·**2**H^+ in the **1**·**2** sample could be excluded. The remarkably higher chemical shift of the main HN^+ species relative to those of **2**H^+ and **2**·**2**H^+ can be interpreted as a strong hint for the formation of a hydrogen bond to the phosphoric acid. Therefore, this species was assigned as NH(**1**·**2**$_{O\cdots HN}$) (Figure 1c). Furthermore, the DOSY value, $D_{corr} = 1.39 \times 10^{-10}\ m^2 s^{-1}$, obtained for NH(**1**·**2**$_{O\cdots HN}$) clearly indicates the formation of a complex.

The calculated hydrodynamic volume of NH(**1**·**2**$_{O\cdots HN}$) is puzzling at a first glance, because it is two times larger than that of OH(**1**·**2**$_{OH\cdots N}$). However, if one considers that toluene was used as the solvent and that, in contrast to OH(**1**·**2**$_{OH\cdots N}$), NH(**1**·**2**$_{O\cdots HN}$) is a contact ion pair, which offers additional possibilities for electrostatic and cation–π interactions, this greater hydrodynamic volume is in accordance with the assignment of the two complex species. Another possible explanation for the increased volume (see the Supporting Information) is stabilization by additional acid molecules, as previously found by Limbach and co-workers.[18]

Thus, the combined NMR spectroscopic results discussed above show that the complex **1**·**2** does not form solely a hydrogen-bonded species or a contact ion pair in solution, but that both species OH(**1**·**2**$_{OH\cdots N}$) and NH(**1**·**2**$_{O\cdots HN}$) coexist simultaneously. Furthermore, minor amounts of the free protonated aldimine NH(**2**H^+) are present.

In synthetic applications, variations in reactivity have been reported for aldimines and differently substituted ketimines upon modification of the electron density of the imine moiety.[2–5] Therefore, we investigated the effect of an aldimine versus a ketimine as well as the effect of different substituents in the ketimine on the ratio of the hydrogen-bonded species to the contact ion pair in these Brønsted acid/imine complexes. To elucidate the influence of ketimines, we chose the structurally closest complex **1**·**3**; for the investigation of substituent effects, the complex **1**·**4** was selected additionally (Scheme 1).

Again, the ^{1}H NMR spectra of **1**·**3** and **1**·**4** showed one averaged signal each for the acidic proton at 300 K (for spectra, see the Supporting Information). Low-temperature measurements in combination with the spectroscopic assignment procedures described above again revealed the coexistence of three species, OH(**1**·**3**/**4**$_{OH\cdots N}$), NH(**1**·**3**/**4**$_{O\cdots HN}$), and NH(**3**/**4**H^+), in both samples (Figure 3). However, the low-temperature ^{1}H NMR spectra of **1**·**3** and **1**·**4** showed that the absolute chemical shift differences and the ratio of the OH(**1**·**X**$_{OH\cdots N}$), NH(**1**·**X**$_{O\cdots HN}$), and NH(**X**H^+) species vary

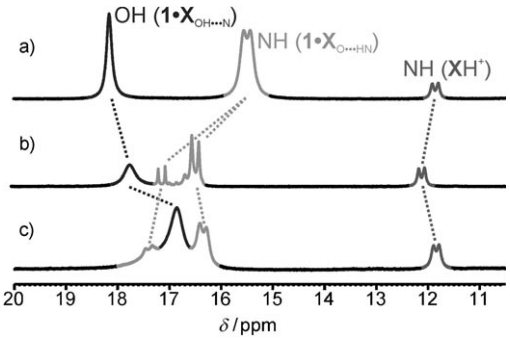

Figure 3. ^{1}H NMR spectra of the different imine–catalyst complexes in [D_8]toluene at 600 MHz: a) **1**·**2** at 240 K; b) **1**·**3** at 220 K; c) **1**·**4** at 210 K. The best chemical shift dispersion and the best line widths of the proton signals were detected at different temperatures for the three samples.

 © 2011 Wiley-VCH Verlag GmbH & Co. KGaA, Weinheim

according to the properties of the imine (see Figure 3 and Table 1).

In **1·2**, the chemical shift difference between OH(**1·2**$_{OH\cdots N}$) and NH(**1·2**$_{O\cdots HN}$) was the largest ($\Delta\delta = 2.66$ ppm). In the ketimine sample **1·3**, the chemical shift difference between OH(**1·3**$_{OH\cdots N}$) and NH(**1·3**$_{O\cdots HN}$) was decreased to $\Delta\delta =$ 1.76 ppm (weighted average of the two NH(**1·3**$_{O\cdots HN}$) species), and in **1·4**, the signals for the different subspecies OH(**1·4**$_{OH\cdots N}$) and NH(**1·4**$_{O\cdots HN}$) even overlap. This stepwise decrease in the $\Delta\delta(^1H)$ values indicates a decrease in the hydrogen-bond strengths within the three complexes, whereby **1·2** > **1·3** > **1·4**. According to the outstanding and very detailed studies of Limbach and co-workers on the strength of hydrogen bonds to an enzymatic cofactor,[7–10] such a decrease in hydrogen-bond strength should correlate with an increase in the ^1H and ^{15}N chemical shift values and a decrease in the $^1J_{H,N}$ values of the NH(**1·X**$_{O\cdots HN}$) species. Indeed, these trends fit perfectly with those observed for NH(**1·2**$_{O\cdots HN}$) and the two NH(**1·3**$_{O\cdots HN}$) species (Table 2).

Table 1: Relative amounts of OH(**1·X**$_{OH\cdots N}$) and NH(**1·X**$_{O\cdots HN}$) in the different samples **1·2**, **1·3**, and **1·4** at 220 K.

Sample	OH(**1·X**$_{OH\cdots N}$)	NH(**1·X**$_{O\cdots HN}$)
1·2	0.33	0.67
1·3	0.42	0.58
1·4	0.61	0.39

Table 2: Hydrogen-bond characteristics of the three complexes **1·2**, **1·3**, and **1·4**.

Complex	$\Delta\delta(^1H)$[a] [ppm]	$\delta(^1H)$[b] [ppm]	$\delta(^{15}N)$[b] [ppm]	$^1J_{H,N}$[b] [Hz]	H-bond strength
1·2[c]	2.66	15.50	75.9	86.0 ± 1.0	
1·3[d]	1.33	16.28	77.3	84.5 ± 0.2	
1·3[d]	0.64	16.97	79.0	83.8 ± 0.2	
1·4[e]	0.56	16.13	n.d.	n.d.	
1·4[e]	−0.56	17.25	n.d.	n.d.	

[a] $\Delta\delta(^1H) = \delta(OH(\mathbf{1\cdot X}_{OH\cdots N})) - (NH(\mathbf{1\cdot X}_{O\cdots HN}))$. [b] The value for NH(**1·X**$_{O\cdots HN}$) is given. [c] At 240 K. [d] At 220 K. [e] At 210 K. n.d. = not determined.

Thus, the different species found for the investigated Brønsted acid/imine complexes are hydrogen-bonded complexes with varying hydrogen-bond strengths in different stages of the proton-transfer reaction. In accordance with this concept,[19] the ratios of the OH(**1·X**$_{OH\cdots N}$) and NH(**1·X**$_{O\cdots HN}$) species also vary (Table 1). In **1·2**, which has the strongest hydrogen bonds, the proton-transfer reaction is most pronounced, and the highest amount of NH(**1·2**$_{O\cdots HN}$) was also observed. Samples **1·3** and **1·4** showed decreasing amounts of NH(**1·3/4**$_{O\cdots HN}$) in agreement with the decreased hydrogen-bond strength indicated by the NMR spectroscopic parameters discussed above.

Next, we investigated the influence of concentration and temperature on the appearance of the different hydrogen-bonded species to estimate the relative amounts of OH(**1·X**$_{OH\cdots N}$) and NH(**1·X**$_{O\cdots HN}$) species under experimental conditions used in Brønsted acid catalyzed reactions. Dilution experiments with **1·2** showed no influence of the absolute concentration on the ratio of OH(**1·X**$_{OH\cdots N}$) to NH(**1·X**$_{O\cdots HN}$) within the experimentally accessible concentration range (for data, see the Supporting Information). In contrast, integration of the ^1H NMR signals of the different species in **1·2**, **1·3**, and **1·4** at different temperatures showed pronounced temperature effects on the relative amounts of OH(**1·X**$_{OH\cdots N}$) and NH(**1·X**$_{O\cdots HN}$) (Figure 4).[20] In all samples, exclusively linear temperature dependencies were observed within the whole temperature range, in which integration was possible because of sufficient chemical shift dispersion.

Figure 4 shows that in general at low temperatures, the ion pairs NH(**1·X**$_{O\cdots HN}$) are stabilized, whereas at increasing temperatures, the hydrogen-bonded complexes OH(**1·X**$_{OH\cdots N}$) become favored. This effect might be explained by additional stabilizing cation–π interactions with the aromatic rings as flexibility is decreased[21,22] and/or improved electrostatic compensation in higher aggregated complexes. Both hypotheses are experimentally corroborated by the considerably higher hydrodynamic volume of NH(**1·2**$_{O\cdots HN}$)

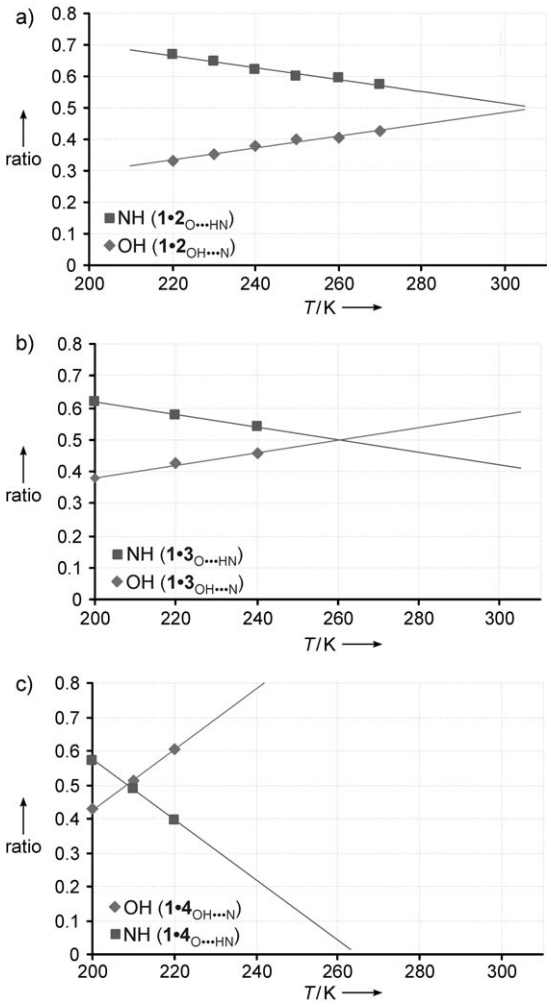

Figure 4. Extrapolation of the temperature dependence of the amounts of OH(**1·X**$_{OH\cdots N}$) and NH(**1·X**$_{O\cdots HN}$) in a) **1·2**; b) **1·3**; c) **1·4**.

 © 2011 Wiley-VCH Verlag GmbH & Co. KGaA, Weinheim

relative to that of OH($\mathbf{1{\cdot}2}_{OH\cdots N}$) (see the Supporting Information). In detail, for **1·2** and **1·3**, different ratios of ion pairs to hydrogen-bonded complexes but similar temperature-dependent slopes were detected (see Figure 4 and Table 1). Samples **1·2** and **1·3** have deviating hydrogen-bond strengths but identical aromatic substituents. Thus, the relative amounts of OH($\mathbf{1{\cdot}X}_{OH\cdots N}$) and NH($\mathbf{1{\cdot}X}_{O\cdots HN}$) at 220 K fit well with the hydrogen-bond strengths, and the similar slopes seem to be caused by the identical aromatic substituents and their π–π interactions.[23,24] In contrast, in **1·4** with the electron-withdrawing CF_3 substituent, the decrease in the amount of NH($\mathbf{1{\cdot}4}_{O\cdots HN}$) and the increase in the amount of OH($\mathbf{1{\cdot}4}_{OH\cdots N}$) with increasing temperature are much stronger than for **1·2** and **1·3**. These significantly steeper slopes might be caused by stronger intermolecular π–π interactions of the electron-deficient aromatic ring of the imine, for example, with the electron-rich solvent toluene. The strong increase in the amount of the NH($\mathbf{1{\cdot}4}_{O\cdots HN}$) species at very low temperatures seems to indicate that either these π–π interactions or cation–π interactions enable partial electron transfer to the imine. This interaction may enhance the basicity of the imine, in analogy with the well-known concept of charge-transfer complexes. This interpretation in terms of intermolecular interactions is in accordance with the rapid loss of such interactions at slightly elevated temperatures, because it is estimated that above 260 K exclusively OH($\mathbf{1{\cdot}4}_{OH\cdots N}$) is present (Figure 4c). We therefore concluded that the OH species is the reactive intermediate for this particular substrate.

In summary, we have been able to demonstrate that NMR spectroscopy is the method of choice to clearly distinguish between the activation modes of hydrogen bonding and ion pairing in Brønsted acid catalysis. Before this study, it was assumed that full protonation of the imine resulted in the formation of an ion pair, which would subsequently react with a nucleophile. However, our experiments clearly show that besides ion pairing, hydrogen bonding exists. The relative hydrogen-bond strength in OH($\mathbf{1{\cdot}X}_{OH\cdots N}$) (**2** > **3** > **4**) and the relative amount of OH($\mathbf{1{\cdot}X}_{OH\cdots N}$) at room temperature (**4** > **3** ≈ **2**) show that both hydrogen-bond strength and the amount of the OH species are decisive for the reaction. Furthermore, the ratio between hydrogen bonding and ion pairing (OH, NH) can be manipulated readily by simply introducing substituents with different electronic properties. These results provide insight into the different activation modes in Brønsted acid catalysis and are expected to guide the development of more efficient catalytic systems.

Received: February 24, 2011
Published online: June 3, 2011

Keywords: activation · Brønsted acids · imines · NMR spectroscopy · organocatalysis

[1] For reviews on Brønsted acid catalysis, see: a) T. Akiyama, *Chem. Rev.* **2007**, *107*, 5744–5758; b) T. Akiyama, J. Itoh, K. Fuchibe, *Adv. Synth. Catal.* **2006**, *348*, 999–1010; c) M. S. Taylor, E. N. Jacobsen, *Angew. Chem.* **2006**, *118*, 1550–1573; *Angew. Chem. Int. Ed.* **2006**, *45*, 1520–1543; d) A. G. Doyle, E. N. Jacobsen, *Chem. Rev.* **2007**, *107*, 5713–5743; e) H. Yamamoto, N. Payette in *Hydrogen Bonding in Organic Synthesis* (Ed.: P. M. Pihko), Wiley-VCH, Weinheim, **2009**, pp. 73–140; f) D. Kampen, C. M. Reisinger, B. List, *Top. Curr. Chem.* **2010**, *291*, 395–456.

[2] For recent reviews on binol phosphoric acids, see: a) M. Terada, *Chem. Commun.* **2008**, 4097–4112; b) M. Terada, *Synthesis* **2010**, 1929–1982; c) M. Terada, *Bull. Chem. Soc. Jpn.* **2010**, *83*, 101–119; d) A. Zamfir, S. Schenker, M. Freund, S. B. Tsogoeva, *Org. Biomol. Chem.* **2010**, *8*, 5262–5276.

[3] For early reports on the application of binol-derived phosphoric acids as highly efficient catalysts, see: a) T. Akiyama, J. Itoh, K. Yokota, K. Fuchibe, *Angew. Chem.* **2004**, *116*, 1592–1594; *Angew. Chem. Int. Ed.* **2004**, *43*, 1566–1568; b) D. Uraguchi, M. Terada, *J. Am. Chem. Soc.* **2004**, *126*, 5356–5357.

[4] For recent examples from our research group, see: a) M. Rueping, E. Sugiono, F. R. Schoepke, *Synlett* **2010**, 852–865; b) M. Rueping, E. Sugiono, T. Theissmann, A. Kuenkel, A. Kockritz, A. Pews-Davtyan, N. Nemati, M. Beller, *Org. Lett.* **2007**, *9*, 1065–1068; c) M. Rueping, E. Sugiono, S. A. Moreth, *Adv. Synth. Catal.* **2007**, *349*, 759–764; d) M. Rueping, E. Sugiono, F. R. Schoepke, *Synlett* **2007**, 1441–1446; e) M. Rueping, A. P. Antonchick, *Org. Lett.* **2008**, *10*, 1731–1734; f) M. Rueping, T. Theissmann, S. Raja, J. W. Bats, *Adv. Synth. Catal.* **2008**, *350*, 1001–1006; g) M. Rueping, A. P. Antonchick, *Angew. Chem.* **2008**, *120*, 10244–10247; *Angew. Chem. Int. Ed.* **2008**, *47*, 10090–10093; h) M. Rueping, A. P. Antonchick, E. Sugiono, K. Grenader, *Angew. Chem.* **2009**, *121*, 925–927; *Angew. Chem. Int. Ed.* **2009**, *48*, 908–910; i) M. Rueping, F. Tato, F. R. Schoepke, *Chem. Eur. J.* **2010**, *16*, 2688–2691; j) M. Rueping, M.-Y. Lin, *Chem. Eur. J.* **2010**, *16*, 4169–4172; k) M. Rueping, T. Theissmann, *Chem. Sci.* **2010**, *1*, 473–476; l) M. Rueping, C. Brinkmann, A. P. Antonchick, I. Atodiresei, *Org. Lett.* **2010**, *12*, 4604–4607; m) M. Rueping, E. Merino, R. M. Koenigs, *Adv. Synth. Catal.* **2010**, *352*, 2629.

[5] W. Schrader, P. P. Handayani, J. Zhou, B. List, *Angew. Chem.* **2009**, *121*, 1491–1494; *Angew. Chem. Int. Ed.* **2009**, *48*, 1463–1466.

[6] a) Y. Cohen, L. Avram, L. Frish, *Angew. Chem.* **2005**, *117*, 524–560; *Angew. Chem. Int. Ed.* **2005**, *44*, 520–554; b) P. S. Pregosin, *Pure Appl. Chem.* **2009**, *81*, 615–633.

[7] S. Sharif, G. S. Denisov, M. D. Toney, H.-H. Limbach, *J. Am. Chem. Soc.* **2007**, *129*, 6313–6327.

[8] S. Sharif, E. Fogle, M. D. Toney, G. S. Denisov, I. G. Shenderovich, G. Buntkowsky, P. M. Tolstoy, M. Chan-Huot, H.-H. Limbach, *J. Am. Chem. Soc.* **2007**, *129*, 9558–9559.

[9] S. Sharif, D. Schagen, M. D. Toney, H.-H. Limbach, *J. Am. Chem. Soc.* **2007**, *129*, 4440–4455.

[10] M. Chan-Huot, S. Sharif, P. M. Tolstoy, M. D. Toney, H.-H. Limbach, *Biochemistry* **2010**, *49*, 10818–10830.

[11] R. M. Gschwind, M. Armbrüster, I. Z. Zubrzycki, *J. Am. Chem. Soc.* **2004**, *126*, 10228–10229.

[12] G. Federwisch, R. Kleinmaier, D. Drettwan, R. M. Gschwind, *J. Am. Chem. Soc.* **2008**, *130*, 16846–16847.

[13] For a study on the hydride, hydrogen, proton, and electron affinity of imines in acetonitrile, see: a) X.-Q. Zhu, Q.-Y. Liu, Q. Chen, L.-R. Mei, *J. Org. Chem.* **2010**, *75*, 789–808; for studies on the electrophilicity of iminium ions derived from secondary amines, see: b) H. Mayr, A. R. Ofial, *Tetrahedron Lett.* **1997**, *38*, 3503–3506; c) S. Lakhdar, T. Tokuyasu, H. Mayr, *Angew. Chem.* **2008**, *120*, 8851–8854; *Angew. Chem. Int. Ed.* **2008**, *47*, 8723–8726.

[14] For NMR spectroscopic studies of iminium ions derived from secondary amines, see: a) C. Rabiller, J. P. Renou, G. J. Martin, *J. Chem. Soc. Perkin Trans 2* **1977**, 536–541; b) H. Mayr, A. R. Ofial, E.-U. Wuerthwein, N. C. Aust, *J. Am. Chem. Soc.* **1997**, *119*, 12727–12733; for NMR spectroscopic studies on protonat-

 © 2011 Wiley-VCH Verlag GmbH & Co. KGaA, Weinheim

ed imines, see: c) R. Knorr, K. Ferchland, *Liebigs Ann.* **1995**, 419–425; d) M. Bissonnetteh, H. Le Thanh, D. Vocelle, *Can. J. Chem.* **1985**, *63*, 2298–2302; e) G. M. Sharma, O. A. Roels, *J. Org. Chem.* **1973**, *38*, 3648–3651.

[15] Deviations from the 1:1 ratio between **1** and the imine lead to an extreme acceleration of the chemical exchange of the acidic proton, which prevents the NMR spectroscopic detection of individual hydrogen-bonded species even at low temperatures.

[16] The unusually small coupling constant of 69.5 Hz for NH(**2**H$^+$) is probably a result of partial decoupling caused by pronounced exchange with the two complex species observed in NOESY spectra at 240 K.

[17] C. Detering, P. M. Tolstoy, N. S. Golubev, G. S. Denisov, H.-H. Limbach, *Dokl. Phys. Chem.* **2001**, *379*, 191–193.

[18] a) N. S. Golubev, S. N. Smirnov, V. A. Gindin, G. S. Denisov, H. Benedict, H.-H. Limbach, *J. Am. Chem. Soc.* **1994**, *116*, 12055–12056; b) S. N. Smirnov, N. S. Golubev, G. S. Denisov, H. Benedict, P. Schah-Mohammedi, H.-H. Limbach, *J. Am. Chem. Soc.* **1996**, *118*, 4094–4101.

[19] T. Steiner, *Angew. Chem.* **2002**, *114*, 50–80; *Angew. Chem. Int. Ed.* **2002**, *41*, 48–76.

[20] The amount of the solvent-separated protonated imine NH-(**X**H$^+$) remained constant in all samples.

[21] D. A. Dougherty, *Science* **1996**, *271*, 163–168.

[22] J. C. Ma, D. A. Dougherty, *Chem. Rev.* **1997**, *97*, 1303–1324.

[23] J. Santos, B. Grimm, B. M. Illescas, D. M. Guldi, N. Martin, *Chem. Commun.* **2008**, 5993–5995.

[24] S. Viel, L. Mannina, A. Segre, *Tetrahedron Lett.* **2002**, *43*, 2515–2519.

 © 2011 Wiley-VCH Verlag GmbH & Co. KGaA, Weinheim